



ELSEVIER

Journal of Chromatography A, 917 (2001) 29–42

JOURNAL OF  
CHROMATOGRAPHY A

www.elsevier.com/locate/chroma

## New family of glutathionyl-biomimetic ligands for affinity chromatography of glutathione-recognising enzymes

S.C. Melissis<sup>a</sup>, D.J. Rigden<sup>b</sup>, Y.D. Clonis<sup>a,\*</sup>

<sup>a</sup>Laboratory of Enzyme Technology, Department of Agricultural Biotechnology, Agricultural University of Athens, 75 Iera Odos Street, GR-11855 Athens, Greece

<sup>b</sup>National Centre of Genetic Resources and Biotechnology, Cenargen/Embrapa, S.A.I.N. Parque Rural, Final W5, Asa Norte, 70770-900, Brasilia, Brazil

Received 26 October 2000; received in revised form 12 February 2001; accepted 13 February 2001

### Abstract

Three anthraquinone glutathionyl-biomimetic dye ligands, comprising as terminal biomimetic moiety glutathione analogues (glutathionesulfonic acid, *S*-methyl-glutathione and glutathione) were synthesised and characterised. The biomimetic ligands were immobilised on agarose gel and the affinity adsorbents, together with a nonbiomimetic adsorbent bearing Cibacron Blue 3GA, were studied for their purifying ability for the glutathione-recognising enzymes, NAD<sup>+</sup>-dependent formaldehyde dehydrogenase (FaDH) from *Candida boidinii*, NAD(P)<sup>+</sup>-dependent glutathione reductase from *S. cerevisiae* (GSHR) and recombinant maize glutathione *S*-transferase I (GSTI). All biomimetic adsorbents showed higher purifying ability for the target enzymes compared to the nonbiomimetic adsorbent, thus demonstrating their superior effectiveness as affinity chromatography materials. In particular, the affinity adsorbent comprising as terminal biomimetic moiety glutathionesulfonic acid (BM1), exhibited the highest purifying ability for FaDH and GSTI, whereas, the affinity adsorbent comprising as terminal biomimetic moiety methyl-glutathione (BM2) exhibited the highest purifying ability for GSHR. The BM1 adsorbent was integrated in a facile two-step purification procedure for FaDH. The purified enzyme showed a specific activity equal to 79 U/mg and a single band after sodium dodecylsulfate–polyacrylamide gel electrophoresis analysis. Molecular modelling was employed to visualise the binding of BM1 with FaDH, indicating favourable positioning of the key structural features of the biomimetic dye. The anthraquinone moiety provides the driving force for the correct positioning of the glutathionyl-biomimetic moiety in the binding site. It is located deep in the active site cleft forming many favourable hydrophobic contacts with hydrophobic residues of the enzyme. The positioning of the glutathione-like biomimetic moiety is primarily achieved by the strong ionic interactions with the Zn<sup>2+</sup> ion of FaDH and Arg 114, and by the hydrophobic contacts made with Tyr 92 and Met 140. Molecular models were also produced for the binding of BM1 and BM3 (glutathione-substituted) to GST I. In both cases the biomimetic dye forms multiple hydrophobic interactions with the enzyme through binding to a surface pocket. While the glutathione moiety of BM3 is predicted to bind in the crystallographically observed way, an alternative, more favourable mode seems to be responsible for the better purification results achieved with BM1. © 2001 Elsevier Science B.V. All rights reserved.

**Keywords:** Affinity chromatography; Affinity adsorbents; Biomimetic ligands; Molecular modelling; Dyes; Enzymes; Formaldehyde dehydrogenase; Glutathione reductase; Glutathione transferase; Triazines

\*Corresponding author. Tel.: +30-1-529-4311; fax: +30-1-529-4307.

E-mail address: clonis@aua.gr (Y.D. Clonis).

## 1. Introduction

Protein separation methods based on the molecular affinity found in biological systems have found wide application in the laboratory and on larger scale for the purification of several commercially important macromolecules [1–3]. The fundamental principle of affinity chromatography is the use of the specific properties of biologically active substances to form stable, specific and reversible complexes [1,2]. The efficiency of an affinity system is determined by its specificity, capacity and stability and these three features are more or less dependent upon the nature of the affinity ligand [1–3].

Since the discovery of the specific interaction of the triazine dye Cibacron Blue 3GA (CB36A) with various enzymes and proteins, there has been a considerable expansion in the application of reactive commercial dyes to protein purification (for recent reviews see [4,5]). Their application is only limited by their moderate selectivity. To overcome this limitation, several rational attempts have been made with the aim of increasing the specificity of dye-ligands for target enzymes [4]. By far, the most successful approach is based on the biomimetic dye concept, according to which new dyes that mimic natural ligands of the targeted proteins are designed, after substitution of the terminal aminobenzene sulfonate moiety of Cibacron Blue 3GA for a substrate-mimetic moiety [4,6,7]. These ligands may be considered as being bifunctional since are recognised by several dehydrogenases as chimeric pseudo-substrates, with the anthraquinone moiety mimicking the natural coenzyme and the biomimetic moiety acting as a substrate-mimetic analogue. The biomimetic dyes exhibit increased purifying ability and specificity and provide useful tools for designing simple and effective purification protocols. This approach has been successfully used in the case of (keto)carboxyl group-recognising enzymes, such as formate [7], L-lactate [6], and L-malate [8] dehydrogenases.

The approach of designing biomimetic dye-ligands can be either empirical, by substituting large number of substrate-mimetic structures to the parent dye [7,9], or rational, by employing molecular modelling techniques and the three-dimensional (3D) structure of the target enzyme to predict the optimum biomimetic ligand structure [6,10–12]. The latter

approach has found successful application to the design of biomimetic dye-ligands for L-malate dehydrogenase [12] and L-lactate dehydrogenase [6].

In the present study we examine the biomimetic concept with the view of designing, synthesising and studying a new family of glutathionyl-biomimetic ligands and respective affinity adsorbents. These immobilised biomimetic dyes are analogues of the parent dichlorotriazine dye Vilmafix Blue A-R (VBAR), bearing as biomimetic moiety glutathione-like structures. The new biomimetic adsorbents were studied for their purifying ability for three glutathione-dependent enzymes,  $\beta$ -nicotinamide-adenine dinucleotide ( $\text{NAD}^+$ )-formaldehyde dehydrogenase (FaDH) from *Candida boidinii*, glutathione reductase from *S. cerevisiae* and recombinant glutathione S-transferase I from maize.

In the absence of an efficient purification protocol for FaDH, we further applied a glutathionyl-biomimetic adsorbent to the development of a facile purification procedure for the enzyme. The study of FaDH purification is justified by the biotechnological potential of this enzyme. For example, it is used as an analytical tool for the determination of formaldehyde and glutathione in food and other biological materials [13].

## 2. Experimental

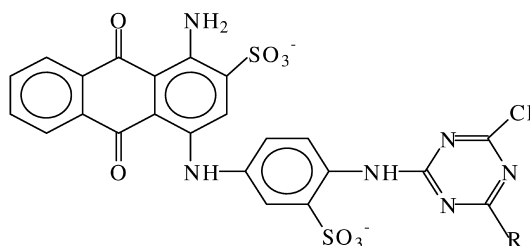
### 2.1. Materials

*Candida boidinii* strain ATCC 32195 was purchased from the American Type Culture Collection.  $\text{NAD}^+$  (crystallised lithium salt ca. 100%), crystalline bovine serum albumin (fraction V) and reduced glutathione were obtained from Boehringer Mannheim (Germany). Formaldehyde, glutathione-sulfonic acid, S-methylglutathione, CB3GA, lipophilic Sephadex LH-20 and DEAE-Sepharose CL6B were obtained from Sigma (St. Louis, MO, USA). The agarose chromatography gel Ultrogel A6R, was a gift from Dr. Boschetti, BioSeptra (France).

### 2.2. Synthesis and purification of glutathionyl-biomimetic dye-ligands

Biomimetic dye ligands (Table 1, structures 1–3) were synthesised by nucleophilic substitution at the

Table 1  
Characteristics of glutathionyl-biomimetic dyes (1–3) and Cibacron Blue 3GA (CB3GA)



Dye-ligand (-R)	$M_r$ (sodium salt)	$m\epsilon$ ( $1\text{ mM}^{-1}\text{ cm}^{-1}$ ) in water	$\lambda_{\text{max}}$ (nm) in water
(1) $-\text{HNC}_{10}\text{H}_{15}\text{N}_2\text{O}_6\text{SO}_3^-$	999.6	7.9	606
(2) $-\text{HNC}_{10}\text{H}_{14}\text{N}_2\text{O}_6\text{SCH}_3$	965.6	9.1	605
(3) $-\text{SC}_{10}\text{H}_{14}\text{N}_2\text{O}_6\text{NH}_2$	951.6	9.8	613
(4) $-o\text{-HNBenZSO}_3^-$ (CB3GA)	839.5	12.6	622

dichlorotriazine ring of the parent dye (VBAR) by the N-terminal amino group of the glutathione analogues (glutathionesulfonic acid and *S*-methylglutathione, structures 1, 2) or by the  $-\text{SH}$  group of glutathione (structure 3), as follows: solid commercial VBAR (227 mg, 0.2 mmol dichloroform, purity 61.3%, w/w) was added to water (10 ml, 25°C) and the solution was slowly introduced under stirring to a solution (20 ml) of the glutathione analogues (0.2 mM) or glutathione (1 mM). The pH was adjusted to 7.5 for the glutathione analogues and to 3.0 for the glutathione, and kept at this value throughout the reaction. The reaction time was varied depending on the nucleophile structure (25°C): 2.5–3 h for the glutathionesulfonic acid and *S*-methylglutathione and 48 h for the glutathione. The progress of each reaction was followed by TLC using the solvent system: 2-propanol–ammonia–water (7:2:1, v/v). After the reaction was completed (as judged by TLC) the mixture was lyophilised and stored desiccated at 4°C.

Dye purification was achieved by a combination of preparative TLC and LC as follows: lyophilised reaction mixture of each dye (20 mg) was dissolved in water (0.4 ml) and the solution applied on a Kieselgel 60 plate (silica gel 60, 0.2 mm, 20×20 cm, Merck). The plate was developed using the solvent system 2-propanol–ammonia–water (7:2:1, v/v). Following completion of the chromatography, the plate was dried and the band of interest was scraped

off. The desired dye was extracted from the silica gel with water, filtered through a 0.45  $\mu\text{m}$  cellulose membrane filter (Millipore) and lyophilised. The lyophilised material was dissolved in water–methanol (5 ml, 50:50, v/v) and the solution was chromatographed on a lipophilic Sephadex LH-20 column (30×2.5 cm) as described by Labrou and Clonis [14]. The purification of Cibacron Blue 3GA was performed according to a published procedure [14].

### 2.3. Spectroscopic characterisation of dye-ligands

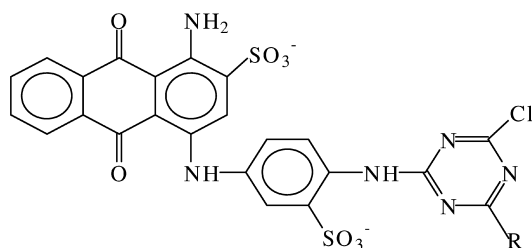
The absorption maxima ( $\lambda_{\text{max}}$ ) and the molar absorption coefficients ( $\epsilon$  values) of the purified dyes were determined as described by Labrou and Clonis [14].

### 2.4. Immobilisation of dye-ligands

To washed crosslinked agarose gel (1 g) was added a solution of purified dye in water (1 ml, the amount of dye is shown in Table 2), followed by NaCl solution (22%, w/v, 0.2 ml). The suspension was tumbled for 30 min at room temperature prior to the addition of solid sodium carbonate (at a final concentration of 1% w/v). The reaction continued under shaking at 60°C. The time of immobilisation reaction was varied depending on the dye-ligand (Table 2). After completion of the reaction, dyed gels were washed sequentially with water (100 ml),

Table 2

Conditions and performance of immobilization reactions for purified dyes on agarose gel



Dye-ligand (-R)	mg dye/g moist gel (in reaction)	Time (h)	$\mu\text{mol dye/g}$ moist gel (in adsorbent)	$\text{m}\epsilon^{\text{a}}$ ( $1 \text{ mM}^{-1} \text{ cm}^{-1}$ )
(1) $-\text{HNC}_{10}\text{H}_{15}\text{N}_2\text{O}_6\text{SO}_3^-$	14.3	49	2.8	5.5
(2) $-\text{HNC}_{10}\text{H}_{14}\text{N}_2\text{O}_6\text{SCH}_3$	11.3	32.5	2.0	6.7
(3) $-\text{SC}_{10}\text{H}_{14}\text{N}_2\text{O}_6\text{NH}_2$	43	60	2.4	7.5
(4) $-o\text{-HNBenZSO}_3^-$ (CB3GA)	6.3	4	2.0	9.2

<sup>a</sup> Determined in medium identical to the one that resulted after acid hydrolysis of the adsorbent [7]. Values were determined from 20  $\mu\text{M}$  dye solutions made in the above medium.

1 M NaCl (50 ml), 50% dimethyl sulfoxide (DMSO) (10 ml), 1 M NaCl (50 ml) and finally water (100 ml). The dyed gels were stored as moist gels in 20% methanol at 4°C.

### 2.5. Determination of immobilised dye concentration

Determination of immobilised dye concentration was achieved according to [7]. The concentration of the immobilised dye was calculated as micromoles of dye per gram moist mass gel, using the molar absorption coefficients shown in Table 2.

### 2.6. Assay of enzyme activity and protein

FaDH, GSHR and GSTI assays were performed at 30°C according to [15,16] and [17], respectively. All assays were performed in a double beam UV–visible spectrophotometer equipped with a thermostated cell holder (10-mm pathlength). One unit of enzyme activity is defined as the amount that catalyses the conversion of 1  $\mu\text{mol}$  of substrate to product per min. Protein concentration was determined by the method of Bradford [18] or by a modified Bradford's methods [19], using bovine serum albumin (fraction V) as standard.

### 2.7. Sodium dodecylsulfate–polyacrylamide gel electrophoresis (SDS–PAGE)

SDS–PAGE was performed according to Laemmli [20] on a 0.75-mm-thick vertical slab gel (10×8 cm) containing 12.5% (w/v) polyacrylamide (running gel) and 2.5% (w/v) stacking gel, using a Hoefer SE 250 dual-slab cell unit. Protein samples, after dialysis against 25 mM Tris–HCl, pH 6.8, were mixed with an equal volume of treatment Tris–HCl buffer (125 mM, pH 6.8) containing SDS (4% v/v), glycerol (20% v/v),  $\beta$ -mercaptoethanol ( $\beta$ -MeSH; 10%, v/v), and bromophenol blue (0.002%, w/v). The samples were incubated at 75°C for 5 min, applied to the wells, and run at a current of 20 mA per gel for 1 h. Protein bands were stained with Coomassie Blue R-250.

### 2.8. Cell cultures

*Candida boidinii* ATCC 32195 stock cultures were maintained in a 50% (v/v) glycerol solution at  $-80^\circ\text{C}$ . The culture medium used was optimised as proposed by Weuster–Botz and Wandrey [21]. The growth of *Candida boidinii* was performed according to Aggelis et al. [22]. Cells were harvested by centrifugation at 4°C (Heraeus Varifuge 20 RS, 10 000 g for 10 min), washed with potassium

phosphate buffer (50 mM, pH 7.6) and stored at  $-20^{\circ}\text{C}$ . *E. coli* M15[pREP4] cells harbouring the expression construct pQE70-GSTI for GSTI expression were grown and induced according to Labrou et al. [23].

### 2.9. Preparation of cell extracts

Cells (4 g paste) were suspended in potassium phosphate buffer (50 mM, pH 7.6, 8 ml) and disintegrated in one passage (flow-rate approx. 0.5 ml/min, 150 bar) using a French-press (capacity 28 ml,  $13\times 5$  cm; Linca Scientific Instruments, Tel Aviv, Israel) which was previously cooled in an ice-bath. After the disintegration cell debris was removed by centrifugation (14 000 g for 30 min,  $4^{\circ}\text{C}$ ). The supernatant was dialysed overnight at  $4^{\circ}\text{C}$  against 5 l of 10 mM potassium phosphate buffer, pH 7.5. The dialysate was clarified through a Millipore cellulose membrane filter (0.45  $\mu\text{m}$  pore size), affording specific activities, typically, as follows: 4.4 units FaDH/mg (13 units FaDH/ml extract, 26 units FaDH/g cell paste), 1.0 unit GSTI/mg (8.4 units GSTI/ml extract, 17 units GSTI/g cell paste) and 0.5 unit GSHR/mg (1.0 unit GSHR/ml extract).

### 2.10. Effect of cycles of press disintegration of *C. boidinii* cells on the extraction of FaDH activity

Cells (5 g paste) were added in potassium phosphate buffer (50 mM, pH 7.6, 10 ml), and press disintegrated in consecutive passages at a flow-rate of approximately 0.5 ml/min (150 bar). Following every passage, a sample (1 ml) was drawn off, centrifuged (14 000 g), and the supernatant assayed for FaDH activity and protein.

### 2.11. Affinity chromatography study of dye adsorbents for binding FaDH activity from *C. boidinii* extract

All procedures were performed at  $4^{\circ}\text{C}$ .

*Step 1: ion-exchange chromatography on DEAE-Sepharose CL6B.* Dialysed extract (10 ml, 130 units FaDH, 29.4 mg protein) was applied to a column of DEAE-Sepharose CL6B anion-exchanger (15 ml,

$3\times 2.5$  cm) previously equilibrated with 10 mM potassium phosphate buffer, pH 7.5. Non-adsorbed protein was washed off with 300 ml equilibration buffer, followed by 300 ml of 50 mM potassium phosphate buffer, pH 7.5. Elution of FaDH activity was carried out with 48 ml potassium phosphate buffer 100 mM, pH 7.5. Collected fractions (8 ml) were assayed for FaDH activity and protein [18]. The fractions with the higher FaDH activity were pooled (24 ml) and the specific activity was determined.

*Step 2: affinity chromatography on dye adsorbents.* FaDH activity eluted from the previous step (24 ml, 101 units FaDH, 2.97 mg protein) was dialysed overnight against 5 litre of 20 mM potassium phosphate buffer, pH 7.5. A sample of the dialysate (1.07 ml, 4.5 units FaDH, 0.13 mg protein) was applied to each analytical column (packed with 0.5 ml of dye adsorbent), previously equilibrated with 20 mM potassium phosphate buffer, pH 7.5. Non-adsorbed protein was washed off with equilibration buffer (5 ml). Bound FaDH was eluted by a mixture of 1 mM  $\text{NAD}^{+}$  and 1 mM reduced glutathione (GSH) in the above buffer (8 ml). Collected fractions (2 ml) were assayed for FaDH activity and protein [19]. The fractions with the higher FaDH activity were pooled and the specific activity was determined.

### 2.12. Affinity chromatography study of dye adsorbents for binding GSHR and GSTI activity from *S. cerevisiae* and *E. coli* extracts

*S. cerevisiae* and *E. coli* extracts were dialysed overnight against 5 l of 20 mM potassium phosphate buffer, pH 7.5. A sample of *S. cerevisiae* dialysate (1.0 ml, 1 units GSHR, 2.1 mg protein) and *E. coli* dialysate (1.0 ml, 8.4 units GSTI, 8.1 mg protein) was applied to each analytical column (packed with 0.5 ml dye adsorbent), previously equilibrated with 20 mM potassium phosphate buffer, pH 7.5. Non adsorbed protein was washed off with equilibration buffer (5 ml). Bound GSHR was eluted by a mixture of 1 mM  $\text{NAD}^{+}$  and 1 mM GSH in the above buffer (5 ml), whereas bound GSTI was eluted by 5 mM GSH (5 ml). Collected fractions (1 ml) were assayed for enzyme activity and protein [18]. The fractions

with the higher activity were pooled and the specific activity was determined.

### 2.13. Purification of FaDH from *C. boidinii* extract on immobilised glutathionesulfonic-VBAR

All procedures were performed at 4°C. FaDH activity eluted from the ion-exchanger was dialysed overnight against 5 l of 20 mM potassium phosphate buffer, pH 7.5. The dialysate (1.07 ml, 4.5 units FaDH, 0.132 mg protein) was applied to a column of glutathionesulfonic-VBAR-agarose (BM1; 0.5 ml) which was previously equilibrated with 20 mM potassium phosphate buffer, pH 7.5. Non-adsorbed protein was washed off with 5 ml equilibration buffer. Bound FaDH was eluted in equilibration buffer containing a mixture of 0.5 mM NAD<sup>+</sup> and 0.5 mM GSH (8 ml) in the same buffer. Collected fractions (2 ml) were assayed for FaDH activity and protein ( $A_{280}$ , except for fractions with NAD<sup>+</sup> and GSH where the protein determined by a modified Bradford's method [18]). Those fractions with higher FaDH activity were pooled (6 ml) and the specific activity was determined.

### 2.14. Molecular modelling of *C. maltosa* FaDH

Since the sequence of *C. boidinii* FaDH is not yet known, the closely related *C. maltosa* FaDH sequence [24] was used. A model of *C. maltosa* FaDH was built using the X-ray crystal structure of human  $\chi\chi$  alcohol dehydrogenase [25]. This structure was chosen as the single template from the large number of available alcohol dehydrogenase structures since, uniquely, it represents a glutathione-dependent enzyme. The 66% sequence identity shared by *C. maltosa* FaDH and human  $\chi\chi$  alcohol dehydrogenase rendered the modelling fairly straightforward. The most favourable position for the single insertion in *C. maltosa* FaDH relative to the template was determined by examination of the structure. Five models of *C. maltosa* FaDH were constructed with Modeller 4 [26], using an alignment made with Clustal W [27], and their packing and solvent exposure characteristics analysed with PROSA II [28]. The model with the best PROSA II overall score was taken as the final model. For inspection of

models and crystal structures we used the program O [29].

### 2.15. Docking of the biomimetic (BM) ligands into the *C. maltosa* FaDH model and into GSTI

The structure of the glutathionyl-biomimetic chimeric ligand BM1 was constructed with the aid of the HICUP database of heterocompounds [30]. The CBD and GTT entries, containing Cibacron Blue and glutathione respectively, were combined. The initial placement of the ligand in the active site of the model was carried out for the individual CB3GA-like and glutathione-like portions. Two sources of information were available to guide the placement. First, the binding of CB3GA to the structurally related enzyme liver alcohol dehydrogenase has been investigated experimentally by X-ray crystallography [31], albeit only to 3.7 Å resolution and with the co-ordinates not deposited in the PDB. The presented comparison of CB3GA and NADH binding to liver alcohol dehydrogenase and the description of the binding mode aided the initial placement of the common portion of CB3GA and BM1. To guide the positioning of the glutathione moiety of BM1, the previously described model of glutathione binding to human  $\chi\chi$  alcohol dehydrogenase was used [25]. While not based on experimental data, the binding model was supported by data from mutant enzymes. Refinement of the initial docking mode was carried out using X-PLOR 3.851 [32].

In a similar way models were produced for possible modes of interaction of BM1 and BM3 with GST I. In the case of BM3, an excellent structural guide was available in the form of the known structure of the enzyme in complex with an atrazine-glutathione conjugate (PDB code 1bye [33]). Since this conjugate and BM3 share the same mode of glutathione linkage, the reasonable assumption was made that the glutathione moiety of BM3 would adopt a binding configuration similar to that seen crystallographically. Rotation of bonds enabled the dye portion of BM3, much larger than the atrazine unit of the known structure, to be favourable located in a hydrophobic pocket on the surface of the enzyme, forming multiple interactions. For modelling of BM1 it was presumed that the large dye unit

would adopt the same favourable conformation as modelled for BM3. The glutathione-mimetic moiety of BM1 therefore adopts a different conformation to that observed experimentally. Analysis of the conformational possibilities, located a pocket into which the glutathione part could be docked. However, with a lack of experimental data for this new glutathione binding mode, and despite the model's ability to explain orders of binding among the glutathionyl-biomimetic dye ligands, the BM1 model must be considered more speculative than the BM3 model.

### 3. Results and discussion

#### 3.1. Biomimetic-dye adsorbent design and synthesis

In the present study three glutathionyl-biomimetic dye-ligands, analogues of the parent anthraquinone dichlorotriazinyl dye VBAR, were designed and synthesized to mimic the natural substrate of the glutathione-dependent FaDH. Each biomimetic dye exhibits two enzyme-recognition moieties: the glutathionyl terminal biomimetic moiety, which mimics the enzyme substrate, and the anthraquinone moiety, which acts as nucleotide coenzyme pseudo-analogue.

The biomimetic dyes were purified to homogeneity in two steps. The initial preparative TLC step was proven to be satisfactory, affording dyes with purity >80%. The second purification step (LC on lipophilic Sephadex LH-20 column) was included in order to remove unwanted salts and other organic impurities, affording dyes with typical purity >95%. Table 1 summarises reaction pH values employed for dye synthesis, molecular mass, molar absorption coefficients ( $\epsilon$ ), and absorption maxima ( $\lambda_{\max}$ ) of purified biomimetic dyes.

The conditions and performance of immobilisation reactions of the dye-ligands are summarised in Table 2. All adsorbents were substituted with dye-ligand at the same level (2.0–2.8  $\mu\text{mol dye/g moist gel}$ ). Equal immobilised dye concentration is an important prerequisite when comparing affinity adsorbents, because wide variations in immobilised ligand concentration influence column capacity and specificity and lead to false interpretation of results [7,8].

#### 3.2. Effect of disintegration procedure on the preparation of *C. boidinii* extract with FaDH activity

The number of passages of cells through the press was examined for its effect on the enrichment of the extract with FaDH activity. Fig. 1 shows the amount of enzyme obtained as a function of the number of cell passages through the press (cycles of disintegration). The optimum number of disintegration cycles was found to be one, leading to extract with the highest specific activity for the target enzyme. More disintegration cycles led to a decrease of FaDH specific activity in the extract, although the amount of the extracted enzyme was slightly increased (about 2–6% after every cycle). A previously published method for FaDH extraction from *C. boidinii*, employed a DynoMill disintegrator and led to a specific activity of 0.37 units/mg [15]. The specific activity of our starting extract is one of the highest reported so far, which is important because an efficient purification method requires the optimisation of all stages in downstream processing [1,2,7].

#### 3.3. Chromatographic study of dye-adsorbents for the purification of glutathione-recognising enzymes

Biomimetic and non-biomimetic adsorbents were

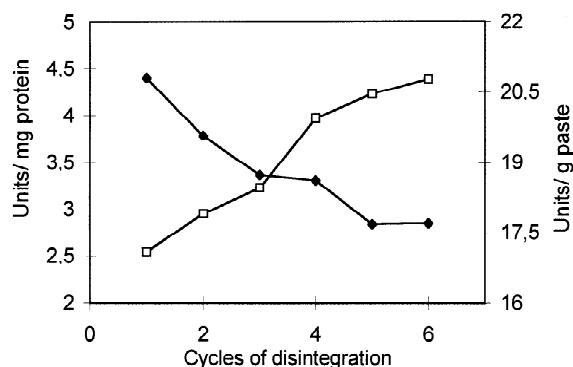


Fig. 1. Effect of number of cycles of press-disintegration of *Candida boidinii* cells on FaDH extraction. Cell paste (0.5 g) is added in 50 mM potassium phosphate buffer, pH 7.6. The suspension is press disintegrated in consecutive cycles at a flow of approximately 0.5 ml/min (150 bar). Following every cycle, a sample is drawn off, centrifuged, and the supernatant assayed for FaDH activity and protein. Units per milligram protein (♦); units per gram cell paste (□).

evaluated for their ability to purify GSHR and GSTI from *S. cerevisiae* and *E. coli* crude extracts, respectively, and FaDH from *C. boidinii* pretreated extract. Table 3 shows the purifying ability of the dye adsorbents after biospecific elution, together with their capacities for the enzymes studied (units/ $\mu\text{mol}$  of immobilised dye). The three new glutathionyl-biomimetic dye adsorbents (BM1–BM3) exhibited substantially higher purifying ability for the target enzymes, compared to the nonbiomimetic control adsorbent (No. 4). Furthermore, adsorbent BM1, which bears as terminal biomimetic moiety glutathionesulfonic acid linked to the triazine ring, displayed the highest purifying ability for FaDH and GSTI, whereas adsorbent BM2, which bears as terminal biomimetic moiety methyl-glutathione, exhibited the highest purifying ability for GSHR. It is most interesting that the GSTI recovered after biospecific elution from the BM1 adsorbent is homogeneous (SDS–PAGE analysis). Furthermore, the purified enzyme exhibited >50% higher purity, compared to the enzyme purified on commercial non-dye glutathionyl-analogue affinity adsorbents [34].

GSH-based affinity adsorbents (e.g. bearing immobilised GSH or GSH analogues) have been successfully used for the isolation of GSH-recognising enzymes [35]. While these adsorbents have found wide application to the purification of GSTs and GSH peroxidases, their application is limited to enzymes that follow ordered (or random) mechanism of substrate binding, with GSH to be the first substrate to bind (e.g. GSTs) [35]. It should be emphasized that the present new biomimetic dye-adsorbents offer the advantage that find application

also in cases where the target enzyme recognizes GSH as the second substrate, and the biocatalyst does not bind to immobilised GSH (e.g. FaDH). The latter is in line with the chimeric nature and function of the new glutathionyl-biomimetic dye ligands.

#### 3.4. Modelling of the interaction between FaDH and BM1

In order to place the dye-adsorbent evaluation results in a structural context, we carried out modelling studies of FaDH and its interaction with BM1. Unfortunately, the *C. boidinii* FaDH sequence is not yet known, but the use of the *C. maltosa* sequence can be readily justified given the close relationship between the two *Candida* species [36].

A certain amount of information was available to guide the initial docking of BM1, from medium-resolution X-ray crystallography in the case of the Cibacron Blue-like portion [31] and from modelling studies in the case of the glutathione moiety [25]. During the modelling process it quickly became apparent that these data could not be perfectly reconciled in a binding mode for BM1 since the distance between the two portions would be too great to enable them to chemically bridge. Placing greater weight on the experimental evidence we, therefore, manually adjusted the glutathione portion of BM1 until it reached bonding distance with the Cibacron Blue-like portion, optimising the interactions with the protein.

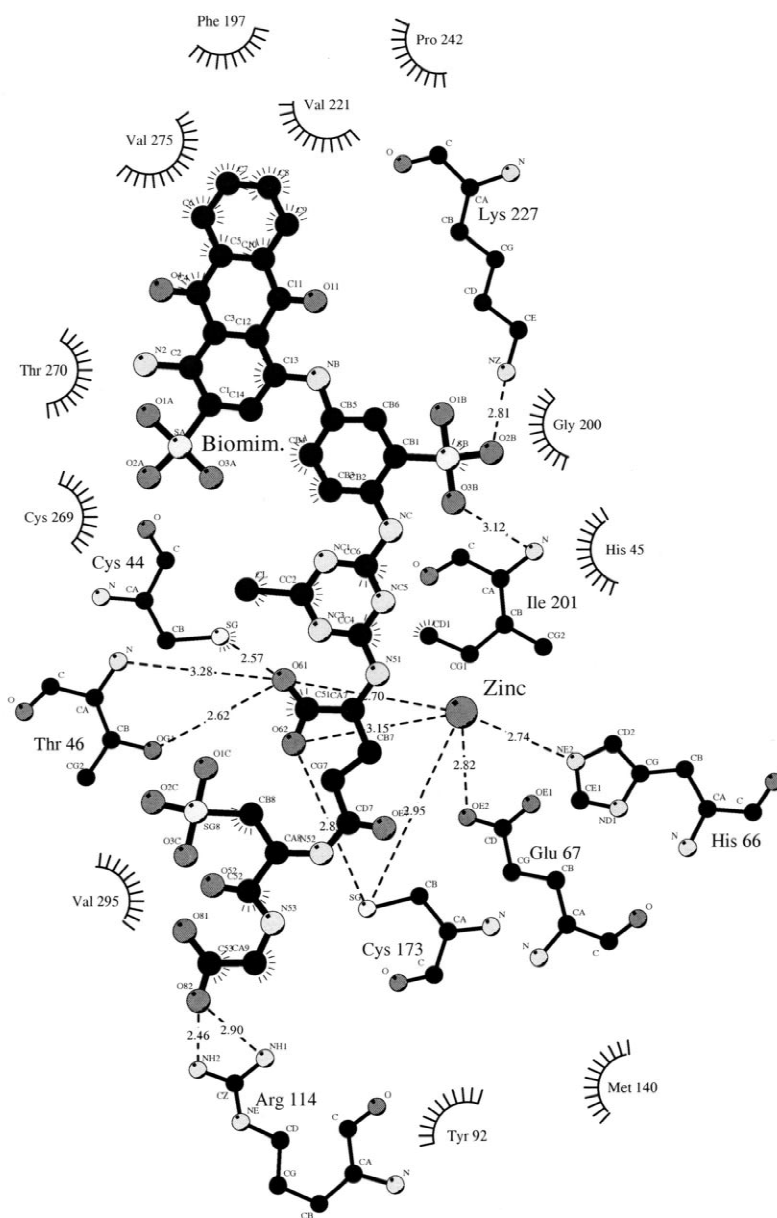
Refinement of the initial position lead to a highly favourable predicted binding mode for BM1 (Figs. 2, 3). The anthraquinone moiety is located deep in the active site cleft forming many favourable hydro-

Table 3  
Evaluation of dye-adsorbents for binding FaDH, GSTI and GSHR activity<sup>a</sup>

Dye-ligand (-R)	Capacity (units/ $\mu\text{M}$ dye)			SA (units/mg)			Purification (-fold)		
	FaDH	GSTI	GSHR	FaDH	GSTI	GSHR	FaDH	GSTI	GSHR
(1) $-\text{HNC}_{10}\text{H}_{15}\text{N}_2\text{O}_6\text{SO}_3^-$	3.0	6.0	0.17	66.3	68.1	3.5	15.0	66.3	7.7
(2) $-\text{HNC}_{10}\text{H}_{14}\text{N}_2\text{O}_6\text{SCH}_3$	4.1	7.2	0.17	62.3	30.5	6.8	14.1	29.7	15.0
(3) $-\text{SC}_{10}\text{H}_{14}\text{N}_2\text{O}_6\text{NH}_2$	2.2	5.2	0.11	60.2	25.2	3.4	13.6	24.5	7.5
(4) $-o\text{-HNBenzSO}_3^-$ (CB3GA)	4.5	1.7	0.10	42.9	11.4	3.1	9.7	11.1	6.8

<sup>a</sup> SA = Specific activity. On each affinity column (0.5 ml), previously equilibrated with 20 mM potassium phosphate buffer, pH 7.5, were applied 4.5 units FaDH, 8.4 units GSTI and 1.0 unit GSHR that have been dialysed in the same equilibration buffer as above (4°C). After the adsorbent was washed with equilibration buffer, elution of bound proteins were effected as described in the Experimental section.





## Key

- |  |                              |  |  |
|--|------------------------------|--|--|
|  | Ligand bond                  |  | Non-ligand residues involved in hydrophobic contact(s) |
|  | Hydrogen bond and its length |  | Corresponding atoms involved in hydrophobic contact(s) |

Fig. 2. A LIGPLOT [37] diagram showing the interactions between BM1 and the *C. maltosa* FaDH in the final modelled structure.

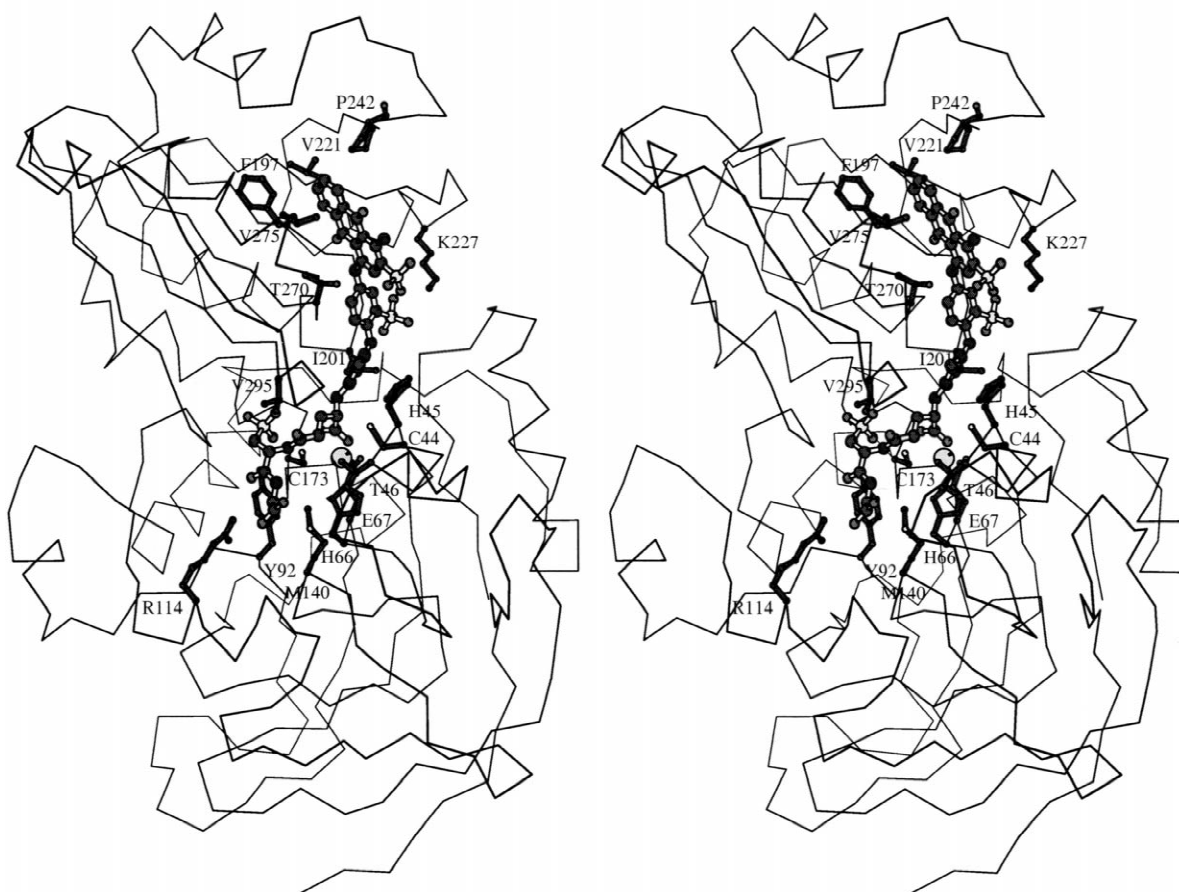


Fig. 3. Stereo MOLSCRIPT [38] diagram of the model of *C. maltosa* FaDH-BM1. The protein is shown only as a  $C_{\alpha}$  trace with the exception of the side chains of those residues interacting with BM1 which are drawn as ball-and-stick. The isolated sphere represents the zinc atom of FaDH.

phobic contacts with, for example, Val275, Phe197, Val221 and Pro242 (Fig. 2). In this way its position resembles that seen experimentally for Cibacron Blue binding to liver alcohol dehydrogenase [31], but differs from the position modelled for the corresponding ring in another biomimetic ligand bound to heart L-lactate dehydrogenase [6]. The sulphonic acid group of the anthraquinone moiety is favourably exposed to solvent (Fig. 3). The sulphonic acid group attached to the diaminobenzene ring occupies a similar position to that of the  $\alpha$ -phosphate of  $NAD^{+}$  in the human  $\chi\chi$  alcohol dehydrogenase structure and can form a favourable ionic interaction with Lys227. As was the case for CB3GA binding to liver alcohol dehydrogenase, the

point of attachment of the triazine ring to the solid matrix is solvent exposed. The position of the glutathione-like biomimetic moiety is rather different to that previously modelled [25], although a strong ionic interaction with Arg 114 can be maintained if this residue is allowed to adopt a different rotamer to that seen in the template crystal structure (Figs. 2,3). Other favourable characteristics of the predicted binding of the glutathione-like part of BM1 to FaDH are the hydrophobic contacts made with Tyr92 and Met140 and the strong interaction of the second carboxylate group with the  $Zn^{2+}$  ion bound by FaDH. Additionally, the sulphonic acid group of the glutathione-like part is favourably solvent-exposed.

The greater affinity of BM1 for FaDH, compared

to CB3GA, is readily explained by the large number of protein interactions predicted for the glutathione-like moiety of BM1 which are absent in the much smaller aminobenzene sulphonate ring correspondingly present in CB3GA. In the case of BM2 and BM3 the unfavourable thermodynamic position of the methyl-group of BM2 in the solvent environment, and the loss of strong interactions formed by Arg114 and Thr46 in the case of BM3, would reduce the affinity of dye-ligands for Fadh.

### 3.5. Modelling of the interaction between GSTI and glutathionyl-biomimetic dye ligands

The results for the purification of GSTI using the present biomimetic dyes may be compared with the known structure of the enzyme in complex with an atrazine–glutathione conjugate (PDB code 1bye [33]). That ligand comprises glutathione bound to the triazinic ring of atrazine through its SH group and,

therefore, most closely resembles BM3 among the dye ligands studied here. Structural examination shows that the additional anthraquinone and sulpho-nated diaminobenzene rings contained in BM3 may be readily accommodated in an additional hydrophobic pocket on the surface of the enzyme (Fig. 4a). Residues Met10, Leu117, Ile118, Met121, Ala176 and Met209 all form hydrophobic interactions with BM3. It is interesting to note that a much better purification results from the use of BM1 than from BM3. Given that, of the triazinyl-dye and glutathionyl moieties it is the latter that is most likely to adopt a different binding mode, this result suggests that the glutathionyl moiety of BM1 may adopt a highly favourable binding mode, different to that crystallographically observed for the glutathione–atrazine conjugate. The possible binding mode shown in Fig. 4b would explain the better results of BM1 compared to BM3. The interactions in Fig. 4b are more numerous than those in Fig. 4a and include

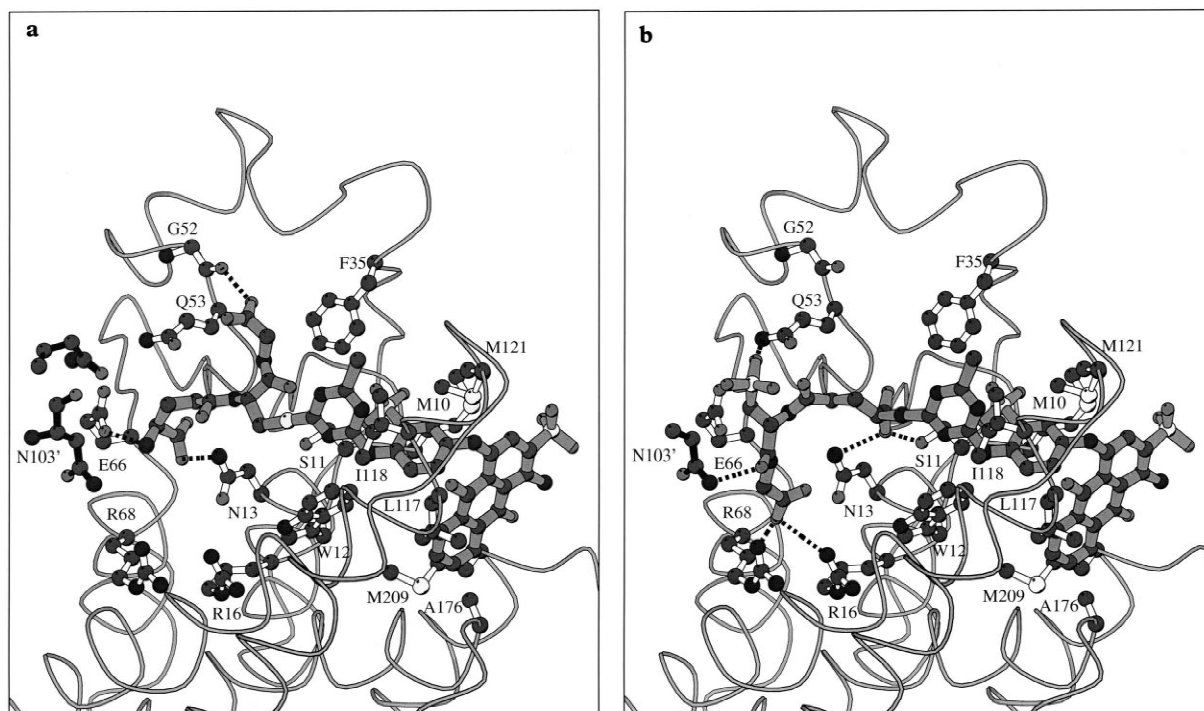


Fig. 4. MOLSCRIPT [38] diagrams of possible docking modes of BM3 (a) and BM1 (b) to GST I based on the structure of GST I complexed with an atrazine–glutathione conjugate (PDB code 1bye; [33]). The protein is shown only as a smooth coil with the exception of the side chains of those residues interacting with BM1 or BM3 which are drawn as ball-and-stick. The ligand bonds are shaded grey while the residue N103' from the adjacent subunit is drawn with black bonds. Possible hydrogen bonds are represented with dotted lines.

strong ionic interactions with residues Arg16 and Arg68. The better performance of BM1 relative to the similar BM2 highlights the importance of the nature of the modification of the sulphur atom of the glutathione moiety. In the model (Fig. 4b) the sulphonic acid group is favourably exposed to solvent and forms a hydrogen bond with Gln53. This interaction would not be possible for BM2, and solvent exposure of its thiol group would be unfavourable.

### 3.6. The purification of FaDH from *C. boidinii* extract on immobilised glutathionesulfonyl-VBAR

Prior to the design of an optimum purification protocol, factors such as the influence of pH in the binding process, and the elution conditions were investigated. Table 4 summarises the effect of pH of the equilibration buffer during adsorption and the effect of concentration of the specific eluent (NAD<sup>+</sup>/glutathione) on FaDH purification. At pH 7.5, BM1 displayed the maximum purifying ability (15-fold), whereas considerable falls is observed under slightly alkaline conditions (Table 4, part a). The pH value of 7.5 was finally chosen for the purification protocol.

The conditions adopted for FaDH specific elution from the BM1 adsorbent are summarised in Table 4, part b. Different concentrations of a mixture of NAD<sup>+</sup> and GSH were tested as biospecific eluents. Elution with 0.5 mM NAD<sup>+</sup> and 0.5 mM GSH led to the highest purification (17.9-fold).

The results of a typical purification run, based on the above optimised procedure, are summarised in Table 5. The specific activity of the purified FaDH was assayed to 79 units/mg and is one of the highest reported so far. The purity of the enzyme preparation was assessed by SDS-PAGE analysis, which showed the presence of a single band corresponding to subunit  $M_r$  of 41 kDa, after Coomassie Blue R-250 staining (Fig. 5).

The majority of highly purified FaDH preparations were originated from methylotrophic yeast with only a few homogeneous enzymes being obtained from other sources. In most cases, the isolation procedures used for the yeast enzymes were multistep and laborious. For example, FaDH from *C. boidinii* has been purified after a combination of anion-exchange and hydroxyapatite chromatography in a four-step procedure, which led to FaDH of specific activity equal to 47.9 units/mg and 75% yield [15]. Another

Table 4  
Effect of pH and elution conditions on the affinity chromatography of *Candida boidinii* FaDH on BM1 biomimetic adsorbent

Method	SA (units/mg)	Purification (-fold)	Recovery(c) (%)
(a) Adsorption at:			
pH 7.0	62.3	14.1	60
pH 7.5	66.3	15.0	76
pH 7.7	63.3	14.3	81
pH 7.9	54.2	12.3	83
(b) Elution with (pH 7.5):			
1 mM NAD <sup>+</sup> /1 mM GSH	66.3	15.0	76
0.5 mM NAD <sup>+</sup> /0.5 mM GSH	78.0	17.9	53
0.1 mM NAD <sup>+</sup> /0.5 mM GSH	62.4	14.2	24
0.1 mM NAD <sup>+</sup> /0.1 mM GSH	40.2	9.1	19

(a) Effect of pH on protein adsorption: on BM1 adsorbent (0.5 ml), previously equilibrated with 20 mM potassium phosphate buffer pH 7.0 to 7.9, was applied 1.07 ml of *C. boidinii* pretreated extract (after DEAE-Sepharose chromatography, 4.5 units FaDH) that has been dialysed in the same equilibration buffer as above. After the adsorbent was washed with equilibration buffer, elution of bound FaDH was effected with 8 ml of a mixture of 1 mM NAD<sup>+</sup> and 1 mM GSH in the same buffer.

(b) Effect of elution conditions on the purification of FaDH: on BM1 adsorbent (0.5 ml), previously equilibrated with 20 mM potassium phosphate buffer, pH 7.5, was applied 1.07 ml *C. boidinii* pretreated extract (after DEAE-Sepharose chromatography, 4.5 units FaDH) that has been dialysed in the same equilibration buffer as above. After the adsorbent was washed with equilibration buffer, elution of bound proteins was effected with 8 ml of the NAD<sup>+</sup>/GSH mixtures shown.

(c) Calculated on the basis of bound and non-washed off FaDH units (100%).

Table 5  
Purification protocol of FaDH from *Candida boidinii* extract on BMI affinity adsorbent<sup>a</sup>

Step	Volume (ml)	Activity (units)	Protein (mg)	Specific activity (units/mg)	Purification (fold)	Yield (%)
Crude extract	10	130	29.4	4.4	1	100
Anion-exchange chromatography (100 mM potassium phosphate buffer elution)	24	101	2.97	34	7.7	77.7
BMI affinity chromatography <sup>b</sup> (NAD <sup>+</sup> /GSH elution)	6	2.29	0.029	79	17.9	51 <sup>b</sup>

<sup>a</sup> Procedures were performed at 4°C. For details see text.

<sup>b</sup> Calculations were based on affinity chromatography of 1.07 ml DEAE–Sepharose pretreated extract (4.5 units, 0.13 mg protein).

purification protocol of FaDH from *Pichia sp.* involved steps such as protamine sulphate treatment and ammonium sulphate fractionation, and anion-exchange, dye-ligand and gel filtration chromatography, leading to a specific activity of 2.09 units/mg [39]. The enzyme has also been purified from rat liver in a two step procedure combining affinity chromatography on a 5'-AMP-agarose column and

chromatofocusing, leading to a specific activity of 2.49 units/mg and 58% yield [40].

In conclusion, in this report we describe the design, synthesis and application of three new glutathionyl-biomimetic ligands and respective adsorbents suitable for the affinity purification of glutathione-recognising enzymes. The affinity purification method described for FaDH, is simple and effective, as it yields pure enzyme suitable for analytical applications. The new biomimetic adsorbents could find application as affinity chromatography tools to the purification of other glutathione-recognising enzymes, with glutathione transferases being the most attractive candidates.

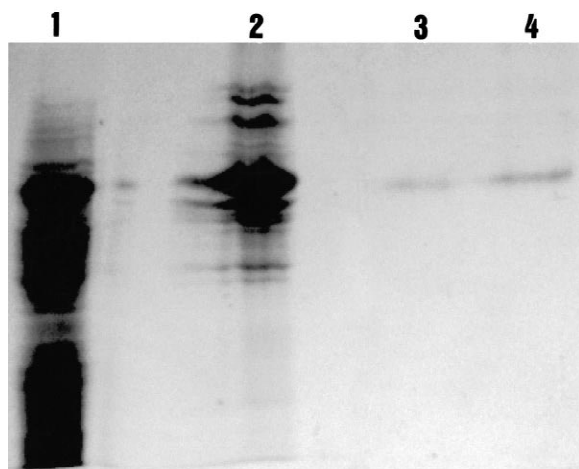


Fig. 5. SDS–PAGE was performed on a 0.75-mm-thick vertical slab gel containing 12.5% (w/v) polyacrylamide (running gel) and 2.5% (w/v) stacking gel. The protein bands were stained with Coomassie Blue R-250. Lanes: 1 = *Candida boidinii* extract (20 µg total protein); 2 = after DEAE–Sepharose anion-exchange chromatography (10 µg total protein); 3, 4 = after affinity chromatography on BMI (1 and 2 µg protein, respectively).

## Acknowledgements

We appreciate the contribution of Dr. G. Aggelis to the preparation of the *C. boidinii* cultures.

## References

- [1] N.E. Labrou, Y.D. Clonis, J. Biotechnol. 36 (1994) 95.
- [2] C. Jones, A. Patel, S. Griffin, J. Martin, P. Young, K. O'Donnell, C. Silverman, T. Porter, I. Chaiken, J. Chromatogr. A 707 (1995) 3.
- [3] G.J. Sofer, J. Chromatogr. A 707 (1995) 23.
- [4] Y.D. Clonis, N.E. Labrou, V.Ph. Kotsira, C. Mazitsos, S. Melissis, G. Gogolas, J. Chromatogr. A 891 (2000) 33.

- [5] N.E. Labrou, Y.D. Clonis, in: M.A. Vijayalakshmi, (Ed.), *Theory and Practice of Biochromatography*, Harwood Academic Publishers, Netherlands, in press.
- [6] N.E. Labrou, E. Eliopoulos, Y.D. Clonis, *Biotechnol. Bioeng.* 63 (1999) 322.
- [7] N.E. Labrou, A. Karagouni, Y.D. Clonis, *Biotechnol. Bioeng.* 48 (1995) 278.
- [8] N.E. Labrou, Y.D. Clonis, *J. Biotechnol.* 45 (1995) 185.
- [9] S.J. Burton, C.V. Stead, C.R. Lowe, *J. Chromatogr.* 455 (1988) 201.
- [10] K. Sproule, P. Morrill, J.C. Pearson, S.J. Burton, K.R. Hejnes, H. Valore, S. Ludvigsen, C.R. Lowe, *J. Chromatogr. B* 740 (2000) 17.
- [11] S.T. Teng, K. Sproule, A. Husain, C. Lowe, *J. Chromatogr. B* 740 (2000) 1.
- [12] N.E. Labrou, E. Eliopoulos, Y.D. Clonis, *Biochem. J.* 315 (1996) 695.
- [13] M. Koivusalo, L. Uotila, *J. Biol. Chem.* 249 (1974) 7653.
- [14] N.E. Labrou, Y.D. Clonis, *Arch. Biochem. Biophys.* 316 (1995) 169.
- [15] H. Schütte, J. Flossdorf, H. Sahm, M.R. Kula, *Eur. J. Biochem.* 62 (1976) 151.
- [16] L. Lopez-Barea, C.-Y. Lee, *Eur. J. Biochem.* 98 (1979) 487.
- [17] A. Caccuri, P. Ascenzi, G. Antonini, M. Parker, A. Oakley, E. Chiessi, M. Nuccetelli, A. Battistoni, A. Bellizia, G. Ricci, *J. Biol. Chem.* 271 (1996) 16193.
- [18] M. Bradford, *Anal. Biochem.* 72 (1976) 248.
- [19] J.C. Bearden Jr., *Biochim. Biophys. Acta* 533 (1978) 525.
- [20] U.K. Laemmli, *Nature (London)* 227 (1970) 680.
- [21] D. Weuster-Botz, C. Wandrey, *Process Biochem.* 30 (1995) 563.
- [22] G. Aggelis, S. Fakas, S. Melissis, Y.D. Clonis, *J. Biotechnol.* 72 (1999) 127.
- [23] N.E. Labrou, D. Rigden, Y.D. Clonis, *Eur. J. Biochem.* 267 (2000) 6657.
- [24] K. Sasnauskas, R. Jomantiene, A. Januska, E. Lebediene, J. Lebedys, A. Janulaitis, *Gene* 122 (1992) 207.
- [25] Z.-N. Yang, W.F. Bosron, T.D. Hurley, *J. Mol. Biol.* 265 (1997) 330.
- [26] A. Šali, T.L. Blundell, *J. Mol. Biol.* 234 (1993) 779.
- [27] J.D. Thompson, D.G. Higgins, T.J. Gibson, *Nucleic Acids Res.* 22 (1994) 4673.
- [28] M.J. Sippl, *Proteins: Structure, Function and Genetics* 17 (1993) 355.
- [29] T.A. Jones, J. Zou, S.W. Cowan, M. Kjeldgaard, *Acta Cryst.* A47 (1991) 110.
- [30] G.J. Kleywegt, T.A. Jones, *Acta Cryst.* D54 (1998) 1119.
- [31] J.-F. Biellmann, J.-P. Samama, C.J. Bränden, H. Eklund, *Eur. J. Biochem.* 102 (1979) 107.
- [32] A.T. Brünger 1999, Available on the WWW at <http://xplor.csb.yale.edu/xplor-info/xploronline.html>.
- [33] L. Prade, R. Huber, B. Bieseler, *Structure* 6 (1998) 1445.
- [34] N.E. Labrou, Y.D. Clonis, unpublished results.
- [35] F. Toribio, E. Martínez-Lara, P. Pascual, J. López-Barea, *J. Chromatogr. B* 684 (1996) 77.
- [36] M.R. Fernandez, J.A. Biosca, A. Norin, H. Jornvall, X. Pares, *FEBS Lett.* 370 (1995) 23.
- [37] A.C. Wallace, R.A. Laskowski, J.M. Thornton, *Protein Eng.* 8 (1995) 127.
- [38] J. Kraulis, *J. Appl. Cryst.* 24 (1991) 946.
- [39] R.N. Patel, C.T. Hou, P. Derelanko, *Arch. Biochem. Biophys.* 221 (1983) 135.
- [40] L. Uotila, M. Koivusalo, Formaldehyde Dehydrogenase, in: A. Larson, S. Orrenius, A. Holmgren, B. Mannervik (Eds.), *Functions of Glutathione: Biochemical, Physiological, Toxicological and Clinical Aspects*, Raven Press, New York, 1983, p. 175.